NOTICE

AVIS

Canada

UNIVERSITY OF ALBERTA

TRANSITIONS TOWARD TURBULENCE IN A CURVED CHANNEL

BY

SHELDON BENJAMIN BLAND

A THESIS

SUBMITTED TO THE FACULTY OF GRADUATE STUDIES AND RESEARCH
IN PARTIAL FUFILLMENT OF THE REQUIREMENTS FOR THE DEGREE OF
MASTER OF SCIENCE.

DEPARTMENT OF MECHANICAL ENGINEERING

EDMONTON, ALBERTA

FALL 1990

Dept. of Mechanical Engineering
University of Alberta
Edmonton, Alberta
Canada T6G 2G8

Warren H. Finlay
Associate Professor
Ph.D., P.Eng.

Phone: (403) 492-4707
FAX: (403) 492-2200
bitnet: userwhf@mts.ucs.ualberta.ca
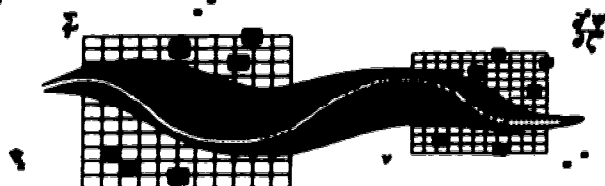
Thursday, September 27, 1990

Graduate Studies and Research
University of Alberta
Edmonton, Alberta

Dear Sir or Madam:

I hereby authorize Sheldon B. Bland to include all material in the joint paper entitled "Transitions toward turbulence in a curved channel" as part of his M.Sc. thesis. (The paper is coauthored by Mr. Bland and myself, and accepted to Phys. Fluids A) .

Sincerely,

W. Finlay

UNIVERSITY OF ALBERTA

RELEASE FORM

NAME OF AUTHOR: Sheldon Benjamin Bland

TITLE OF THESIS: Transitions Toward Turbulence in a Curved Channel

DEGREE: Master of Science

YEAR THIS DEGREE GRANTED: 1990

PERMISSION IS HEREBY GRANTED TO THE UNIVERSITY OF
ALBERTA LIBRARY TO REPRODUCE SINGLE COPIES OF THIS THESIS AND
TO LEND OR SELL SUCH COPIES FOR PRIVATE, SCHOLARLY OR
SCIENTIFIC RESEARCH PURPOSES ONLY.

THE AUTHOR RESERVES OTHER PUBLICATION RIGHTS, AND
NEITHER THE THESIS NOR EXTENSIVE EXTRACTS FROM IT MAY BE
PRINTED OR OTHERWISE REPRODUCED WIHTOUT THE AUTHOR'S
WRITTEN PERMISSION.

R.R. #4, Site 2, Box 4
Edmonton, Alberta
T5E - 5S7

Date: SEPT 28, 1990

UNIVERSITY OF ALBERTA

FACULTY OF GRADUATE STUDIES AND RESEARCH

THE UNDERSIGNED CERTIFY THAT THEY HAVE READ, AND
RECOMMEND TO THE FACULTY OF GRADUATE STUDIES AND RESEARCH
FOR ACCEPTANCE, A THESIS ENTITLED *TRANSITIONS TOWARD*
TURBULENCE IN A CURVED CHANNEL, SUBMITTED BY SHELDON
BENJAMIN BLAND IN PARTIAL FULFILLMENT OF THE REQUIREMENTS
FOR THE DEGREE OF MASTER OF SCIENCE.

Dr. W. H. Finlay

Dr. K. Nandakumar

Dr. L. W. Sigurdson

Dr. R. L. Varty

Date: SEPTEMBER 21, 1990

ABSTRACT

A numerical study of the transitions that occur with increasing Reynolds number in a curved channel with radius ratio $\eta = 0.875$ is performed using spectral simulations of the three-dimensional, incompressible, time-dependent Navier-Stokes equations. Periodic boundary conditions are used in the spanwise and streamwise directions. At Reynolds number $Re = 6.31 Re_c$ temporally periodic wavy (twisting) Dean vortices occur (Re_c is the Reynolds number for the transition from laminar curved channel Poiseuille flow to steady, streamwise oriented Dean vortices). At $Re = 8.84 Re_c$ a three frequency flow is discovered in which two new incommensurate frequencies modulate the wavy vortices. At $Re = 10.10 Re_c$ the two modulation frequencies are phase locked producing a two frequency modulated wavy vortex flow that is similar in some ways to that seen in Taylor - Couette flow. The spatial and temporal characteristics of the modulation frequencies are discussed. Based on the behaviour of other dynamical systems, temporal chaos should ensue once the phase locking at $Re = 10.10 Re_c$ is broken at a higher Reynolds number. Judging from current experimentation with curved channel flow, verification of the flows discovered here may be difficult.

ACKNOWLEDGEMENTS

CONTENTS

LIST OF FIGURES

SYMBOLS AND NOMENCLATURE

Roman Symbols

d Channel spacing.

k_θ Streamwise Fourier wavenumber.

k_z Spanwise Fourier wavenumber.

P CCPF pressure.

p Total pressure.

r Radial coordinate.

r_i Inner radius of channel (convex wall).

r_o Outer radius of channel (concave wall).

r_c Centerline radius of channel.

Re $\bar{U}d/2\nu$, Reynolds number.

Re_θ Critical Reynolds number for axisymmetric Dean vortices.

u $v - V(r)e_\theta$, velocity perturbation from CCPF.

u_θ Streamwise component of u.

u_r Radial component of u.

u_z Spanwise component of u.

$\bar{U}$ Mean streamwise velocity.

v Total velocity vector.

v_θ Streamwise component of v.

v_r Radial component of v.

v_z Spanwise component of v.

V CCPF velocity (streamwise).

z   Spanwise coordinate.

Greek Symbols

β Streamwise wavenumber.

Γ h/d, aspect ratio of channel.

Δp Pressure gradient parameter.

θ Streamwise spatial coordinate.

η r_i/r_o, radius ratio.

λ Spanwise wavelength of vortices.

μ Streamwise wavelength.

ν Kinematic viscosity.

ω Fundamental frequency of wavy and modulated wavy Dean vortex flow.

Other Symbols

CCPF Curved channel Poiseuille flow.

CHAPTER I

INTRODUCTION

The purpose of this work is to numerically study the transition to turbulence of flow through an infinite aspect ratio curved channel.

Until now, four distinct laminar flows were known to exist prior to the onset of turbulence in the curved channel. At low Reynolds numbers the most basic flow exists. This is curved channel Poiseuille flow. As the Reynolds number is increased, curved channel Poiseuille flow becomes centrifugally unstable and axisymmetric streamwise oriented roll cells, known as Dean vortices, develop[1]. Increasing Re further causes the Dean vortices to become unstable to periodic streamwise travelling waves producing either undulating or twisting vortices[2]. In this work the method of Moser and Moin[3] is used to simulate the three dimensional, incompressible, time-dependent, Navier-Stokes equations for curved channel flow with Re above that for stable wavy vortices.

In chapter II, the paper format is used to present the results of this study. An explanation of the curved channel geometry and the parameter range explored appears in section II.1. In II.2 the code used in performing the simulations is described. A flow containing two new incommensurate frequencies, in addition to that due to the original travelling wave, is described in section II.3. The two new frequencies become phase locked at higher Re, giving a flow that is similar to two frequency modulated wavy Taylor vortex flow[4]. A vortex doubling is encountered at higher Re, limiting the extent of the present study. The spatial and temporal characteristics of the new modes are discussed in II.4.

1

The work concludes with chapter III. The transition route outlined thus far for curved channel flow is viewed from a dynamical system perspective. Speculation is made as to what further transitions curved channel flow will undergo before becoming turbulent. As well, difficulties that may be encountered in physically verifying the flows discovered here are briefly discussed.

CHAPTER I REFERENCES

1. W.R. Dean, Proc. R. Soc. Lond. A121, 402 (1928).

2. W.H. Finlay, J.B. Keller, and J.H. Ferziger, J. Fluid Mech. 194, 417 (1988).

3. R.D. Moser, P. Moin and A. Leonard, J. Comput. Phys. 52, 524 (1983).

4. M. Gorman and H.L. Swinney, J. Fluid Mech. 117, 123 (1982).

CHAPTER II

TRANSITIONS TOWARD TURBULENCE IN A CURVED CHANNEL[1]

II.1 Definitions and Background

The channel geometry used in this investigation is shown in Fig. 2.1. The streamwise, spanwise and radial coordinates are defined by θ, z and r respectively. The inner and outer walls have radii r_i and r_o. The channel spacing is $d = r_o - r_i$, and the radius ratio is defined as $\eta = r_i/r_o$. Channels of finite spanwise extent h, will have an aspect ratio $\Gamma = h/d$. All velocities are non-dimensionalized by the bulk streamwise velocity $\overline{U}$, distances are non-dimensionalized by d/2, and time by $d/2\overline{U}$. The Reynolds number Re is defined as $Re = \overline{U}d/2\nu$. Wavy vortices are characterized by spanwise and streamwise wavenumbers $\alpha = \pi d/\lambda$ and $\beta = 2\pi/\mu$, where λ and μ are the spanwise and streamwise wavelengths respectively.

The following regimes have been observed for curved channel flow with infinite, or at least very large, aspect ratio. At low enough Re the flow is azimuthal, except near the ends of a finite aspect ratio channel where single Ekman vortices occur[1]. At the critical $Re = Re_c$ (and critical $\alpha = \alpha_c$) the flow becomes unstable and gives way to streamwise oriented roll cells[2]. Finite aspect ratio effects on this transition are discussed by Finlay and Nandakumar[1]. Much of the previous literature on curved channel flow deals with the neutral stability of the azimuthal flow in infinite aspect ratio channels of arbitrary η. A review of this literature is given by Finlay, Keller, and Ferziger[3]. Finlay

---

[1]. A version of this chapter has been accepted for publication. Bland & Finlay 1990. Physics of Fluids A.

4

et al.[3] examined the stability of axisymmetric Dean vortices to wavy disturbances and performed numerical simulations of curved channel flow for $\eta = 0.975$ and $\alpha = 2.5$. They found that for $Re \geq 1.2Re_c$ Dean vortex flow is unstable to relatively long wavelength or "undulating" travelling waves. For $Re \geq 1.96Re_c$ the axisymmetric Dean vortex flow becomes unstable to short wavelength or "twisting" travelling waves. At higher Re, the linear growth rates for the short wavelength twisting modes were found to be greater than that for long wavelength undulating modes. Experimental evidence for the existence of twisting vortex flow at $\eta = 0.979$ is given by Ligrani and Niver[4]. In recent experiments, twisting and undulating vortex flows have been observed for $\eta = 0.979$ that compare well with numerical computations for the same curvature[5]. When increasing Re from $8.2Re_c$ to $10.9Re_c$ at $\eta = 0.975$, $\alpha = 2.5$, $\beta = 200$, Finlay et al.[3] found vortex doubling where two vortices split to become four. This prevented further investigation of possible transition routes for the chosen η and α. No transitions beyond wavy (periodic) vortex flow were found.

In this investigation, $\eta = 0.875$, $\alpha = 2.5$, $\beta = 30$ are considered. By lowering η, the spanwise wavenumber α, is found to be stable against vortex doubling through a larger number of bifurcations than at $\eta = 0.975$. At $\eta = 0.875$, $Re_c = 52.4$; the transition to twisting vortex flow occurs at $Re \sim 2.6Re_c$[3]. We use a spanwise wavenumber $\alpha = 2.5$ because experimentally $\alpha \sim 2.55$ for $\eta = 0.979$ and $2.14Re_c \leq Re \leq 3.07Re_c$[6], $\alpha \sim 2.17$ at $\eta = 0.99$ and $Re \sim 125Re_c$ for turbulent channel flow[7], and $2.6 \leq \alpha \leq 3.0$ for $\eta = 0.979$ and $2.03Re_c \leq Re \leq 4.53Re_c$[4]. We use a streamwise wavenumber of $\beta = 30$ because infinitesimal nonaxisymmetric streamwise disturbances to Dean vortex flow

have highest linear growth rates near this β when $\eta = 0.875$ and $\alpha = 2.5$[3].

The transitions beyond twisting Dean vortex flow that occur with increasing Re are described in section II.3 and the spatial and temporal characteristics of the new modes are discussed in II.4. In section II.2, the numerical method used to simulate the flow is briefly discussed. Spanwise and streamwise periodicity is imposed; thus, phenomena associated with the end walls of finite aspect ratio channels are not considered. The flow is fully developed with no entrance effects studied.

II.2 Code Implementation

The code employs the method of Moser, Moin and Leonard[8] to obtain three dimensional, time-dependent, incompressible solutions of the Navier-Stokes equations for the curved channel. Periodic boundary conditions in the spanwise and streamwise directions are employed. A pseudo-spectral method based on expansion functions that satisfy the continuity equation and boundary conditions is used. Time advancement is implicit for viscous terms and explicit for nonlinear convective terms. Solution symmetry in the spanwise or streamwise direction is not enforced since previous authors have found in other geometries that asymmetric modes are important in the production of incommensurate frequencies leading to chaos[9]. The computational box contains one spanwise wavelength (one counter-rotating vortex pair) λ, and one streamwise wavelength μ. Spatial resolution is monitored by ensuring that the logarithm of the energy decreases linearly with increasing Fourier wavenumber k_z or k_x up to the highest wavenumber. Constant mass flux is imposed.

The code is a modification of the one used to study wavy Dean vortex flow by

6

Finlay et al.[3], Taylor vortex flow by Moser et al.[8] and turbulent curved channel flow by Moser and Moin[10]. The numerical method was also used by Finlay to study rotating channel flow[11], to test perturbation expansions for curved and rotating channel flows[12], and to study the transition to turbulence in rotating channel flow[13].

II.3 Temporal Spectra

In this section flow simulations performed at $Re = 6.31Re_c$, $8.84Re_c$, $10.10Re_c$, $10.35Re_c$ and $11.36Re_c$ are discussed. During the simulations, the velocity is sampled over time for use in both a stationary and a streamwise travelling reference frame. Power spectra of these time records provide a means of distinguishing flow regimes. Unless otherwise stated, the initial condition for each run is the fully developed flow at the previous, lower Re. Simulations at $Re = 8.84Re_c$ and $10.10Re_c$ using initial conditions containing low amplitude $(10^{-5}\overline{U})$ random noise superimposed on a first order approximation to Dean vortices with a strong $(10\% \ \overline{U})$ nonaxisymmetric perturbation yielded the same equilibrium flows, after long transients. Spatial resolution for each run is as follows: for $Re = 6.31Re_c$ and $8.84Re_c$, $24 \times 33 \times 36$ modes are used in the θ, r and z directions respectively; for $Re = 10.10Re_c$ and $10.35Re_c$, $32 \times 33 \times 40$ resolution is used, and for $Re = 11.36Re_c$, $40 \times 33 \times 40$ is used. The random noise initial condition runs at $8.84Re_c$ and $10.10Re_c$ both use resolutions of $32 \times 49 \times 40$. To remove aliasing errors, the resolution in physical space is 3/2 times the number of modes in transform space in each direction.

All the flows described in this section satisfy shift and reflect symmetry as defined by Marcus[14]:

$$v_r(r,\theta,z,t) - v_r(r,\theta+\pi/\beta,-z,t)$$
$$v_\theta(r,\theta,z,t) - v_\theta(r,\theta+\pi/\beta,-z,t) \qquad \text{(II.1)}$$
$$v_z(r,\theta,z,t) - -v_z(r,\theta+\pi/\beta,-z,t).$$

This symmetry is satisfied to within roundoff even though no such symmetry is enforced.

A portion of the velocity records and power spectra at $Re = 6.31Re_c$, $8.84Re_c$, and $10.10Re_c$ are shown in Fig. 2.2, 2.3, and 2.4 respectively. Only the low frequency portion of the power spectrum is shown in Fig. 2.3 and 2.4. No fundamental frequency components are contained at frequencies higher than those shown. The data shown was obtained at $r \approx r_c - d/4$ and $z \approx \lambda/4$, where $z = 0$ is the average location of the outflow region between adjacent pairs of vortices. Data obtained at other locations and for the other components of velocity are qualitatively no different.

At $Re = 6.31Re_c$, the flow is temporally periodic with frequency $\omega_1 = 2.09 \pm .04$, where $\omega = 2\pi/T$, and T is the nondimensional period of oscillation. (The flow at $Re = 6.31Re_c$ was obtained using fully developed wavy vortices at $Re = 3.16Re_c$ as initial conditions.) When the velocity is sampled in a frame of reference travelling in the streamwise direction at a constant angular velocity, the fundamental, ω_1, is shifted by an amount proportional to the angular velocity. The periodicity of the flow is thus due to a wave travelling down the channel at constant angular velocity $\Omega = \omega_1/\beta$. Formally, the wave satisfies the definition of a travelling wave given by Rand[15]:

$$v(r,(\theta+\Omega\Delta t)\bmod 2\pi/\beta,z,t+\Delta t) - v(r,\theta,z,t). \qquad \text{(II.2)}$$

8

The flow is a twisting vortex flow as defined by Finlay[11] and is qualitatively similar to the twisting vortices observed by Finlay et al.[3] at $\eta = 0.975$.

At $Re = 8.84Re_c$ the flow becomes quasi-periodic with three incommensurate frequencies. The original travelling wave is still present, $\omega_1 = 2.097 \pm .005$, but there are two new modes, $\omega_2 = 0.275 \pm .005$ and $\omega_3 = 0.138 \pm .005$. The two new frequencies remain unchanged in a travelling reference frame. They are also incommensurate; this is most easily seen in the time record of Δp, defined as

$$\Delta p = \frac{\overline{\frac{\partial p}{\partial \theta}} - \frac{\partial P}{\partial \theta}}{\frac{\partial P}{\partial \theta}} \qquad (\text{II.3})$$

where $-(1/r)(\partial p/\partial \theta)$ is the streamwise pressure gradient, $\overline{\partial p/\partial \theta}$ is the value of $\partial p/\partial \theta$ averaged over the computational box and $(-1/r)(\partial P/\partial \theta)$ is the streamwise pressure gradient for laminar (unstable) curved channel Poiseuille flow at the same Re. Due to its travelling wave nature, ω_1 is absent from Δp records. The time records and power spectra of Δp for $Re = 8.84Re_c$ and $10.10Re_c$ are given in Fig. 2.5 and 2.6 respectively. After an initial transient, the beating of ω_2 and ω_3 against each other can be seen in the amplitude oscillation of the time record of Δp for $Re = 8.84Re_c$. The power spectrum of Δp shows ω_2 and ω_3 and their linear combinations. It is expected that ω_2 and ω_3 first appear at different Re. Which appears first however was not determined due to the large amounts of CPU time required for such runs.

The flow at $Re = 10.10Re_c$ is the same as that at $8.84Re_c$ except the two low frequencies, ω_2 and ω_3 have become phase locked. A power spectrum of the velocity,

9

shown in Fig. 2.4, gives $\omega_1 = 2.098 \pm .007$, $\omega_2 = 0.258 \pm .007$, and $\omega_3 = 0.129 \pm$ .007. Within the resolution of the spectra obtained, $\omega_2/\omega_3 = 1.99$ for $Re = 8.84 Re_e$, while for $Re = 10.10 Re_e$ $\omega_2/\omega_3 = 2.00$. The phase locking is most clearly illustrated in the record of Δp given in Fig. 2.6. For $Re = 8.84 Re_e$, ω_2 and ω_3 beat against each other, while at $Re = 10.10 Re_e$, ω_2/ω_3 is precisely two, producing a periodic signal for Δp. The power spectrum of Δp for $Re = 10.10 Re_e$ shows ω_3 as the fundamental frequency, all other peaks except one are integer multiples of ω_3. The very low frequency spike ($\omega = 0.03$) in the Δp spectrum corresponds to the slowly decaying transient in the Δp record. Phase locking has been observed in Rayleigh - Bénard convection[16], and in simple dynamical systems governed by nonlinear ordinary differential equations[17]. In many cases, once two frequencies lock, their ratio remains fixed for a finite range of Re. This is the case with the curved channel, since a run made at $Re = 10.35 Re_e$ is qualitatively the same as at $10.10 Re_e$ with ω_2 and ω_3 still entrained with ratio 2 to 1.

At $Re = 8.84 Re_e$ the alternate initial condition involving random noise mentioned earlier resulted in a long transient (22 periods of ω_3) during which the flow was phase locked just as at $Re = 10.10 Re_e$. After this transient, the flow settled into the same equilibrium three frequency state obtained using $Re = 6.31 Re_e$ as initial condition. The alternate initial condition run at $Re = 10.10 Re_e$ quickly gave the same results as the run using $Re = 8.84 Re_e$ as initial condition.

An exploratory run at $Re = 11.36 Re_e$ performed early in the investigation to determine the character of the parameter range, revealed a vortex doubling phenomenon. The solution at $6.31 Re_e$ was used as initial condition. Early in the run, a vortex splitting

10

and subsequent merging occurred. This is evidenced by the shifting of the dominant energy in the first mode of the spanwise velocity Fourier expansion to the second mode, and then back again. The splitting and merging occurred in about one period of ω_3, which is about equal to ω_3 for Re = 10.10Re$_c$. The amplitude of Δp never settles down and another doubling and merging occurs about 90 periods of ω_1 later (or 17 hours of Cray X-MP CPU time later). Experimentally, Ligrani and Hiver observed splitting and merging[4]. This phenomenon is related to a generalized Eckhaus instability[18].

II.4 Spatial and Temporal Characteristics of Modulated Flow

In this section, the modulated flows at Re = 8.84Re$_c$ and 10.10Re$_c$ are discussed in detail. Both flows are frequency and amplitude modulated. Variation of the flow due to modulation is weak at Re = 8.84Re$_c$, but stronger at 10.10Re$_c$.

Inspection of the spanwise velocity time record at Re = 8.84Re$_c$ reveals that the period between arrivals of the travelling wave oscillates at both ω_2 and ω_3. A record of v_z at Re = 8.84Re$_c$ over 1.5 periods of ω_3 is shown in Fig. 2.7 (a). The velocity has been sampled at every time step, giving a resolution of 0.0143 nondimensional time units $d/2\overline{U}$. From this record the period T of the travelling wave is estimated by taking the difference between the times at which consecutive minimums of v_z occur. The time variation of T is shown in Fig. 2.7 (b). The period of the travelling wave is modulated at ω_2 by about $\pm$ 5% of the average T = 2.996; ω_3 modulates T by approximately an additional 2%. Because periodic streamwise boundary conditions fix the streamwise wavelength, the variation of period implies frequency modulation of the travelling wave.

The companion Δp record to the v_z record at Re = 8.84Re$_c$ is shown in Fig. 2.7

11

(c). Comparing Figs. 2.7 (b) and (c) show that several maxima/minima of Δp occur approximately when there is a minima/maxima of T, though there is not an exact correlation between the two. The minima in the Δp record at $t = 1207$ and $t = 1253$ occur between one to two periods of ω_1 ahead of the corresponding minima in v_z variation and maxima in T.

The spatial variation of the flow at $Re = 8.84 Re_c$ due to ω_2 is seen in contour plots through sections of the channel. In Fig. 2.8 contours of the streamwise perturbation velocity u_θ in a r - z plane averaged over one streamwise wavelength μ are given ($u_\theta = v_\theta - V(r)$ where v_θ is the total streamwise velocity and $V(r)$ is the curved channel Poiseuille flow profile[3]). The plots in Fig. 2.8 (a) and (b) correspond to the times $t = 1193$ and $t = 1203$ in Fig. 2.7 (a separation of roughly one half the period of ω_2). The plot at $t = 1193$ shows a stronger negative perturbation velocity at $z = \lambda/2$ and $r = r_o - d/3$ than at $t = 1203$. This is due to the increased strength of the vortices sweeping more low velocity fluid from near the outer wall into the centre of the channel. The stronger vortices also cause the larger positive perturbation at $z = \lambda/2$ and $r = r_i + d/4$.

Spatially averaged streamwise vorticity contours in the r - z plane are shown in Fig. 2.9. The vortices are stronger at $t = 1193$ than at $t = 1203$. This is seen in the higher vorticity at the vortex centres and larger vorticity gradient close to the outer wall in Fig. 2.9 (a).

The effect of ω_2 on the waviness of the inflow boundary of the vortices can be seen in the contours of the streamwise perturbation velocity in a z - θ plane at $r = r_c$ given in Fig. 2.10. At $t = 1193$ (when the travelling wave has its slowest local phase

12

velocity), the inflow boundary (approximated by the "s" shaped valley running across the contour plots), is flatter than at $t = 1203$. The maximum spanwise excursion of the inflow boundary from its average location is 10% greater when the waviness is maximally enhanced vs. flattened.

Because the power intensity of ω_3 is so weak, temporal variation of the spatial structure of the flow at $Re = 8.84 Re_c$ could not be detected at the frequency ω_3 from visual comparison of plots of the velocity field.

The time records of v_z, T, and Δp over 1.5 periods of ω_3 for $Re = 10.10 Re_c$ are given in Fig. 2.11 (a), (b) and (c) respectively. Again the data has been sampled every time step giving a resolution of $\Delta t = 0.0117$. The amplitude and frequency modulation of the travelling wave is much more pronounced here than at $Re = 8.84 Re_c$. The average period of the travelling wave is modulated at ω_3 by about $\pm 15\%$. The large extrema in the period of the travelling wave coincide with the minima in the Δp record.

The spatial effect of the modulation at $Re = 10.10 Re_c$ is seen in channel section contour plots. In Fig. 2.12, contours of the streamwise perturbation velocity u_θ in a r - z plane averaged over one streamwise wavelength μ are given. The velocity field has been sampled at the times $t = 1057$ and $t = 1081$ in Fig. 2.11 (a separation in time of one half a period of ω_3). Extrema in T, Δp, and v_z occur at these times. The plot sampled at $t = 1081$ (high Δp) shows a much stronger negative perturbation velocity at $z = \lambda/2$ and $r = r_o - d/3$ than at $t = 1057$ (low Δp). Again this is due to the increased strength of the vortices sweeping more low velocity fluid from near the outer wall into the centre of the channel. For $t = 1057$, the region near the inner wall has a nearly uniform

13

positive perturbation, while at t = 1081, the stronger vortices push high velocity fluid from the centre of the channel inward, causing a large positive perturbation island at z = $\lambda/2$ and r = r_i + d/4.

Spatially averaged streamwise vorticity contours in the r - z plane are shown in Fig. 2.13. For t = 1081, the vortices are stronger. This causes higher vorticity at the vortex centres and larger vorticity gradients close to the outer and inner walls, and within the inflow region.

The effect of modulation on the waviness of the inflow boundary of the vortices can be seen in the contours of the streamwise perturbation velocity in a z - θ plane at r ~ r_e given in Fig. 2.14. At t = 1057 (when the travelling wave has its slowest phase velocity), the inflow boundary (approximated by the "s" shaped valley running across the contour plots), is more s-shaped than at t = 1081. Observations of the flow at other times show the inflow boundary waviness is maximally flattened when Δp is a maximum and maximally enhanced when Δp is a minimum. The maximum spanwise excursion of the inflow boundary from its average location is 16% greater when the waviness is maximally enhanced vs. flattened.

It is possible that the two frequency phase locked regime at Re = 10.10Re_c discovered here is similar in nature to modulated wavy Taylor vortex flow. Each state in modulated wavy Taylor vortex flow can be described by a combination of the integers m and k; m is the number of azimuthal waves (β in the curved channel), and k is used to define the phase angle $\Delta\phi$ = 2πk/m between the modulation of successive waves. Because of the imposed periodic boundary conditions in the streamwise direction in this

14

study, the periodic flattening of the travelling wave implies that all waves in the streamwise direction simultaneously flatten. This behaviour is similar to the m/k states in modulated wavy Taylor vortex flow described by Gorman and Swinney[19] for k = 0. However, for the k = 0 state of modulated wavy Taylor vortex flow the s-shaped waves have a faster phase velocity than the flattened waves, which is opposite to what is observed here. To determine whether k ≠ 0 states occur in the curved channel requires that more than one streamwise wavelength be resolved. This is beyond the scope of this study.

In Taylor Couette flow, only one frequency has been found that causes pure modulation of the travelling waves. However, two other flow frequencies have been observed[20]. The first corresponds to a transient mode that appears at higher Re than that for the onset of the first travelling wave, but disappears before the appearance of the modulation frequency. The second corresponds to a broadband component, which marks the onset of chaos, coexisting with the two frequencies of modulated wavy Taylor vortex flow. It is unlikely that either of the two new frequencies found at Re = 8.84Re$_c$ in the curved channel are slowly decaying transients, and clearly none of the spikes in any of the power spectra correspond to broad band components. The alternate initial condition runs, besides supporting the argument that the two new frequencies are not transients, also demonstrate that the states obtained in the simulations have basins of attraction that are not points but are of finite size.

II.5 Summary

In this chapter, flow through a curved channel was simulated using the three

dimensional, incompressible, time dependent, Navier - Stokes equations. At Re = 6.31Re_c twisting vortices (wavy Dean vortices) as discussed by Finlay et al.[3] are obtained. At Re = 8.84Re_c a three frequency flow is discovered in which two nonpropagating oscillations modulate the travelling wave associated with the wavy vortices. At Re = 10.10Re_c the two, new nonpropagating frequencies become phase locked, producing a modulated wavy vortex flow like that observed in Taylor - Couette flow. The two modulation frequencies cause both amplitude and frequency variation of the flow. At Re = 8.84Re_c they enhance and flatten the s-shape of the travelling wave and cause it to travel slower when flattened, faster when enhanced. At Re = 10.10Re_c however, the wave travels faster when flattened, slower when enhanced. In both cases the vortices are stronger when the wave is flattened, weaker when more s-shaped. At Re = 11.36Re_c, a vortex doubling was encountered, limiting the extent of the present study.
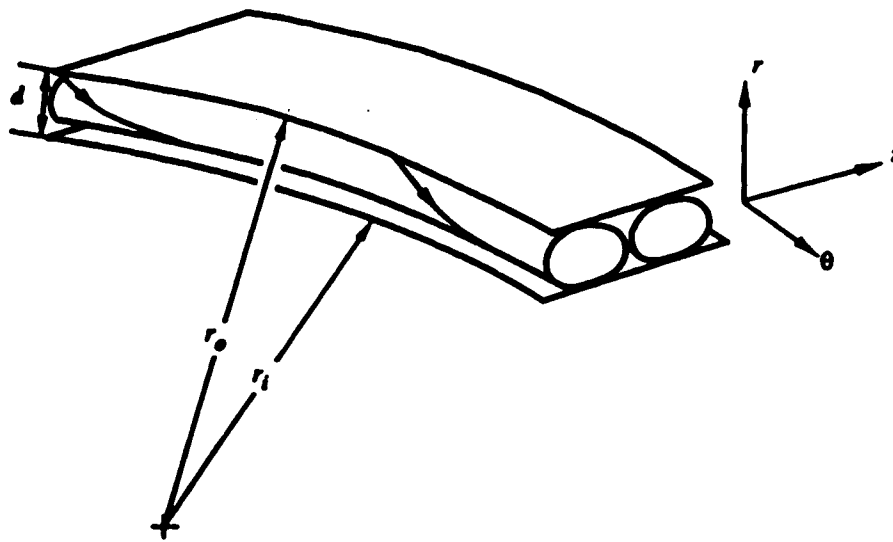
Figure 2.1. A schematic of the curved channel geometry and coordinate system is shown including one pair of axisymmetric Dean vortices.
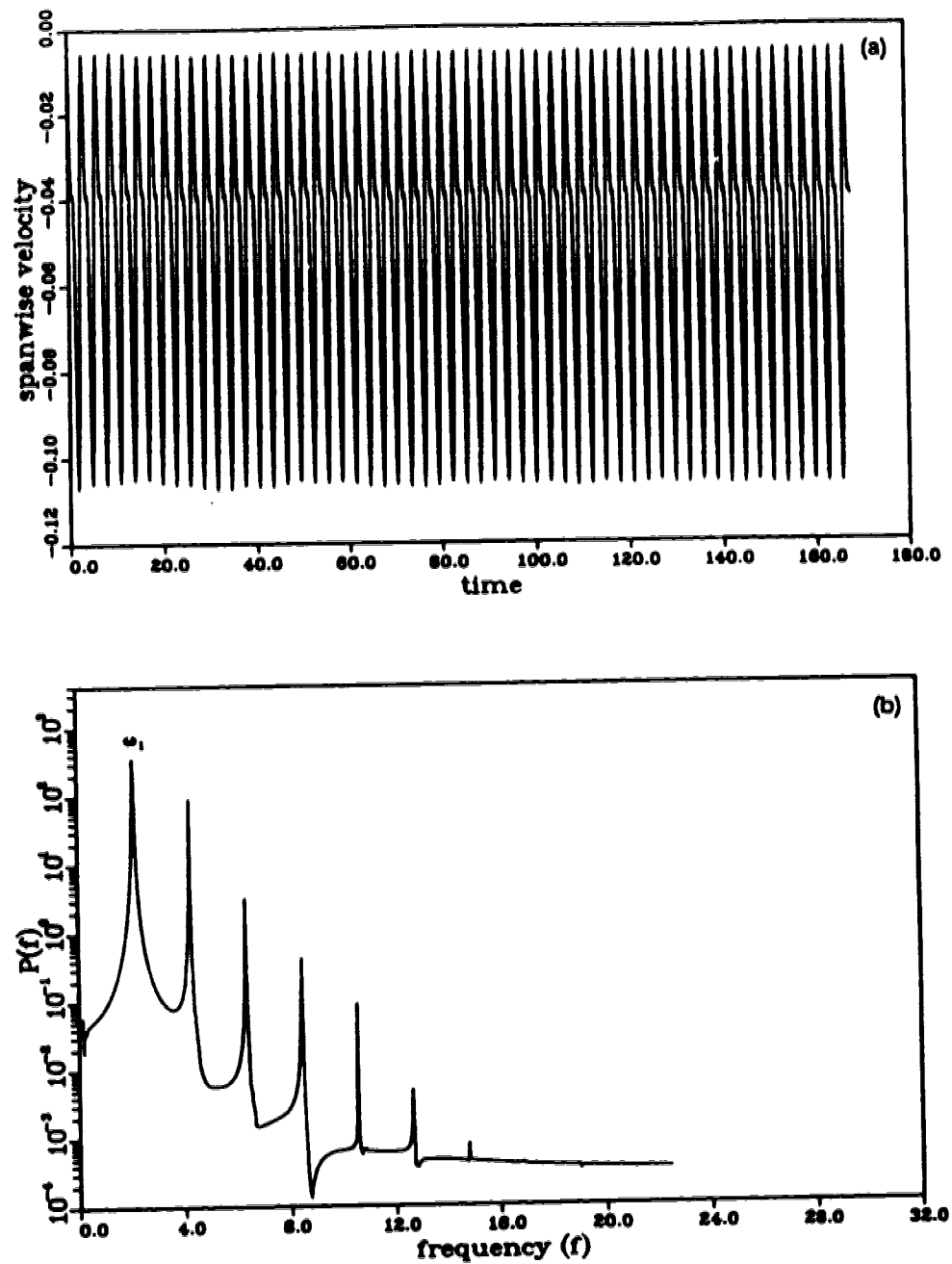
17

Figure 2.2. (a) The time record and (b) the corresponding power spectrum of the spanwise velocity v_z is shown for $Re=6.31Re_c$. The final 168 of 336 nondimensional time units $d/2\bar{U}$ is shown in (a); $\omega_1 = 2.09 \pm .04$.
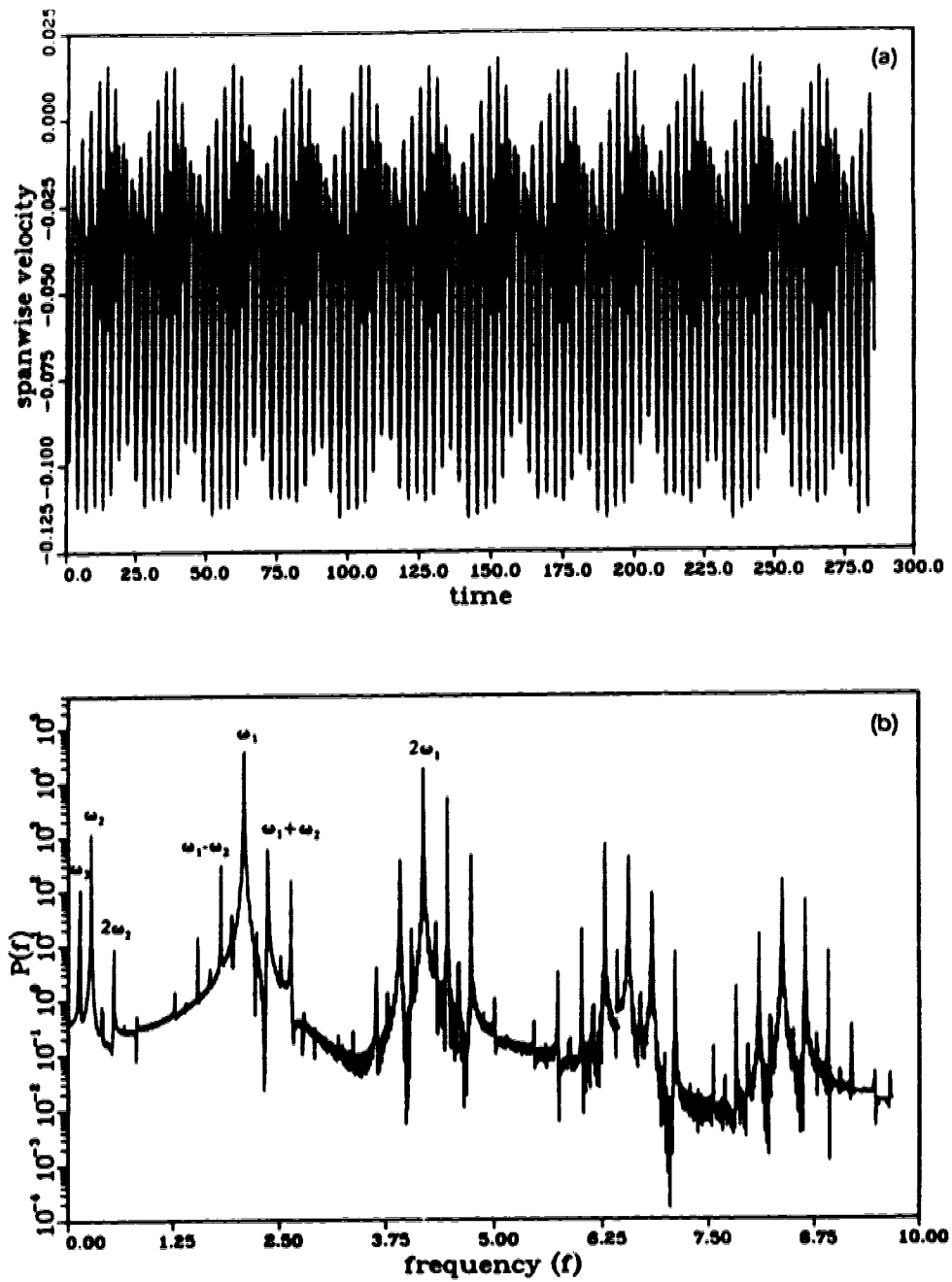
18

Figure 2.3. (a) The time record and (b) the corresponding power spectrum of v_z is shown for $Re = 8.84Re_c$. Only the final 93 out of 420 periods of ω_1 in the run are shown; $\omega_1 = 2.097$, $\omega_2 = 0.275$, $\omega_3 = 0.138$ (all frequencies to within ± .005).

19
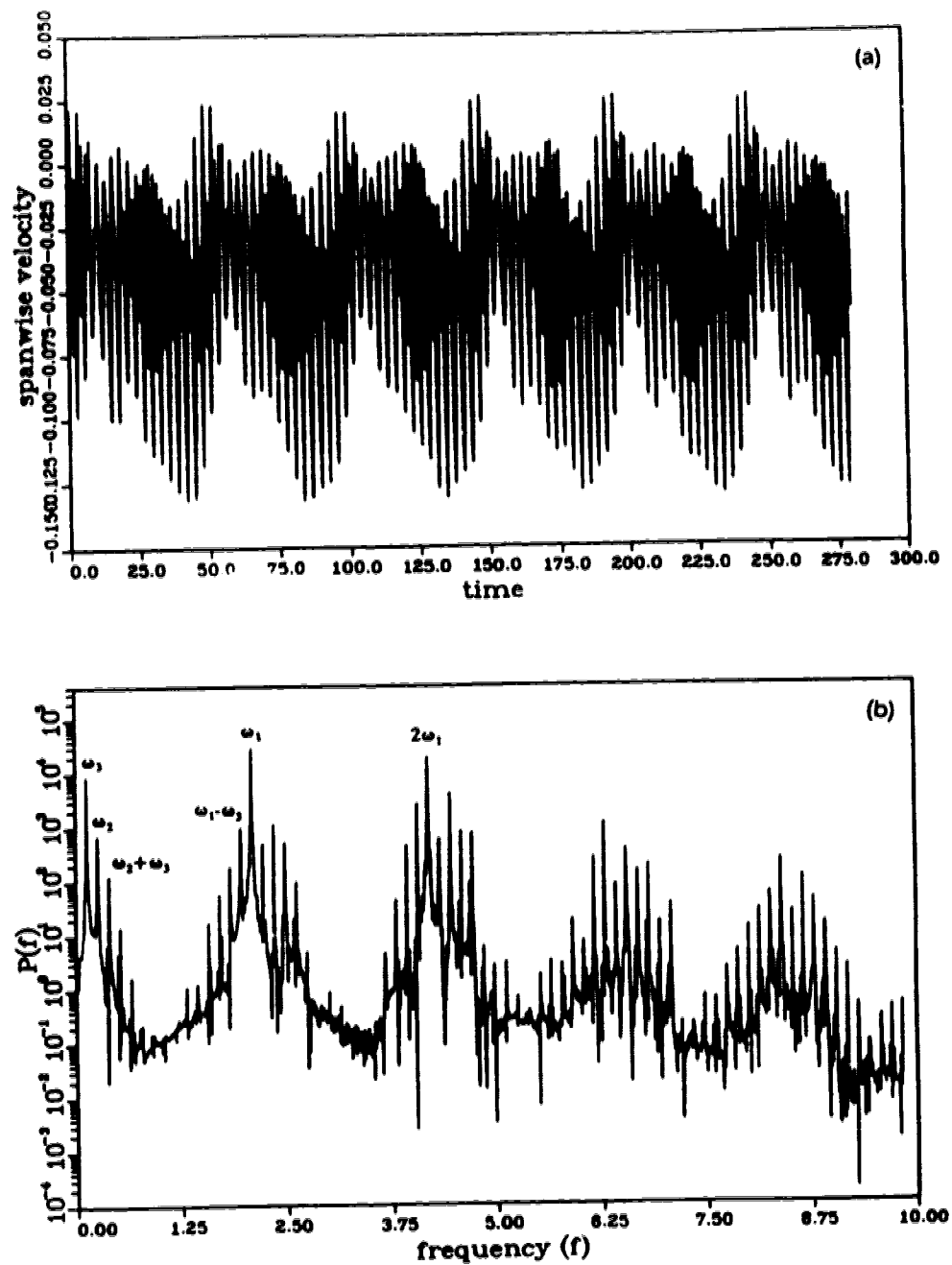
Figure 2.4. (a) The time record and (b) corresponding power spectrum of v_z is shown for $Rc = 10.10Rc_c$. Only 93 out of 300 periods of ω_1 are shown in (a); $\omega_1 = 2.098$, $\omega_2 = 0.258$, $\omega_3 = .129$ (frequencies to within $\pm$ .007).
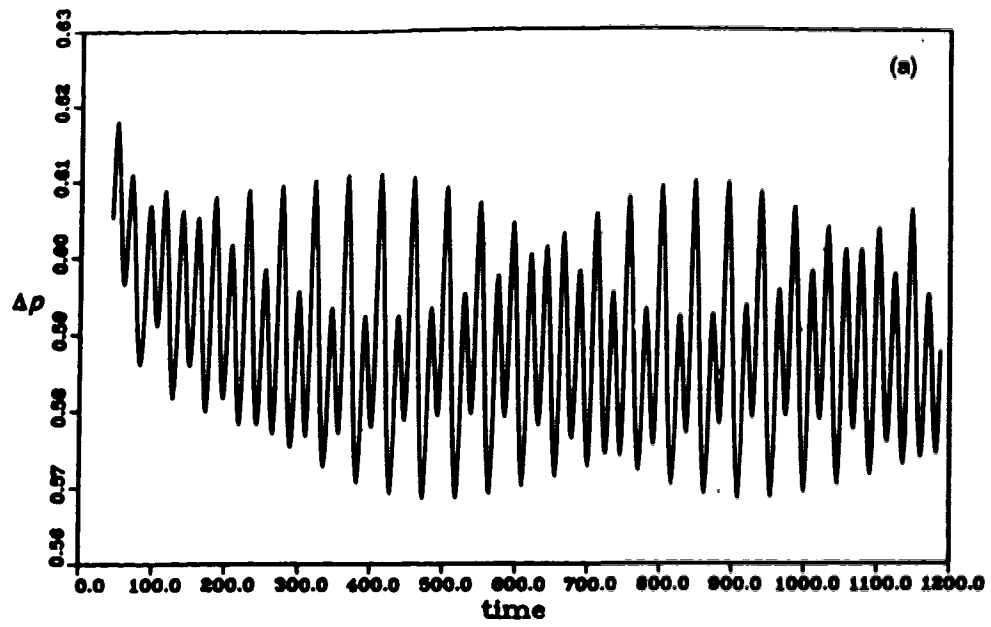
20
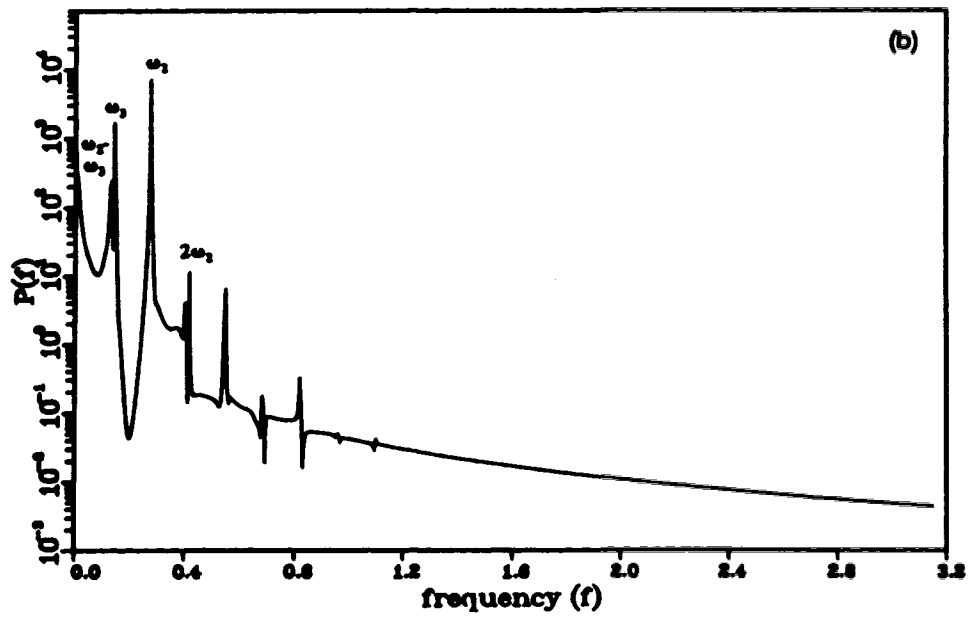
Figure 2.5. (a) The time record and (b) the corresponding power spectrum of Δp is shown
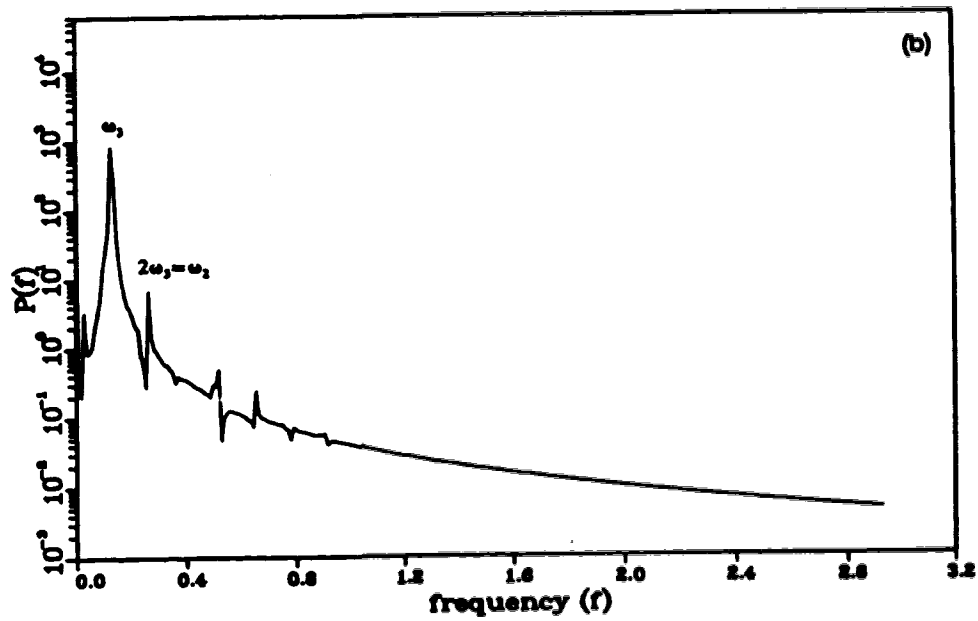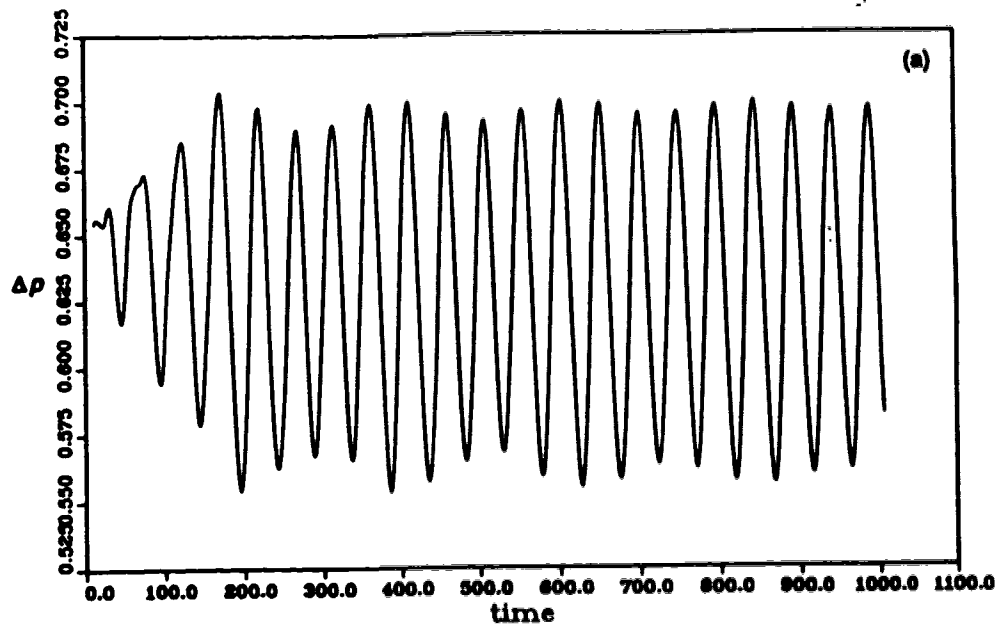
for Re = 8.84 Re$_c$.

21

Figure 2.6. (a) The time record and (b) the corresponding power spectrum of Δp for Re $= 10.10 Re_c$.
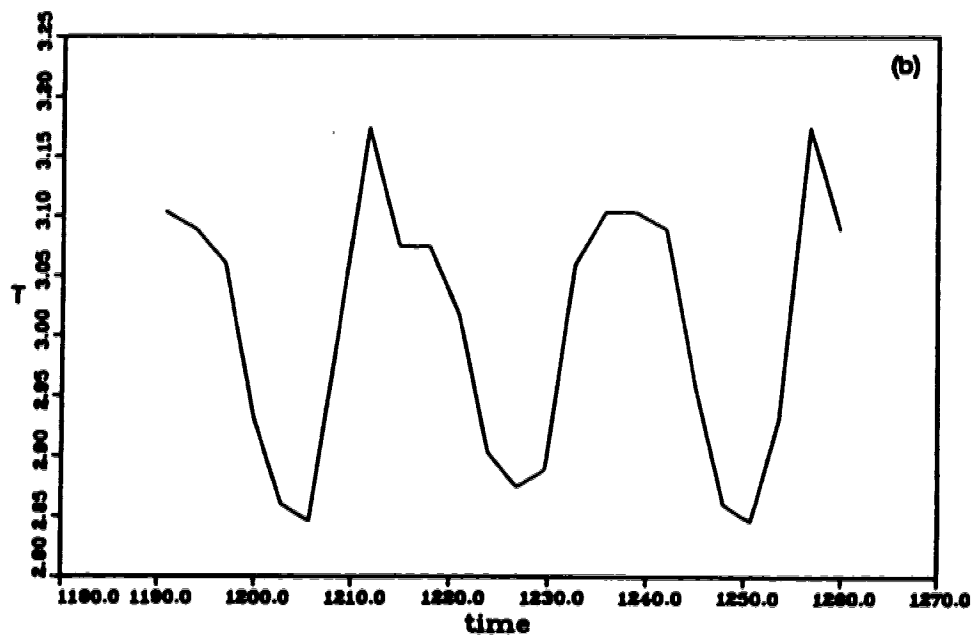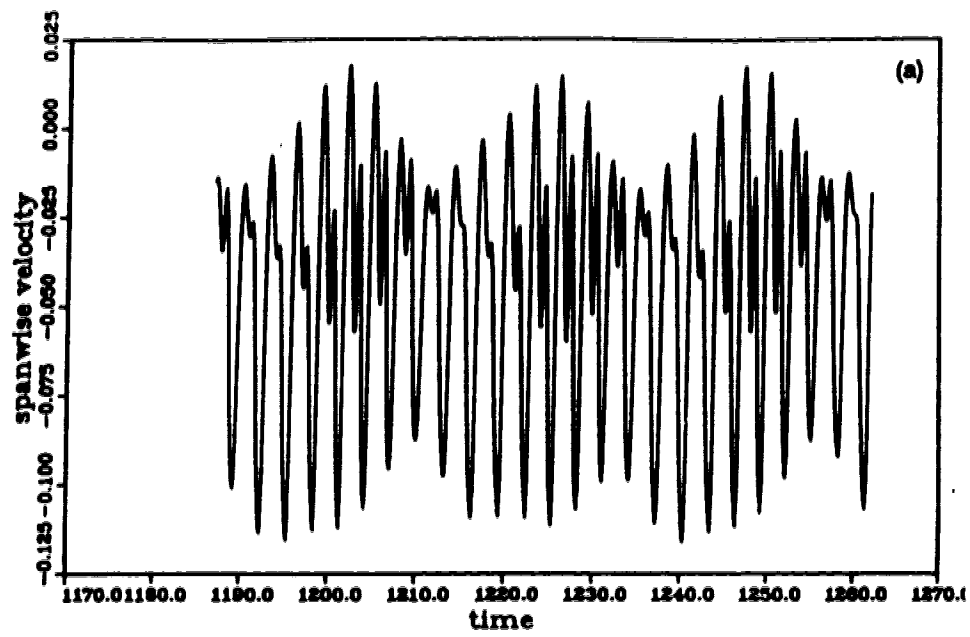
22

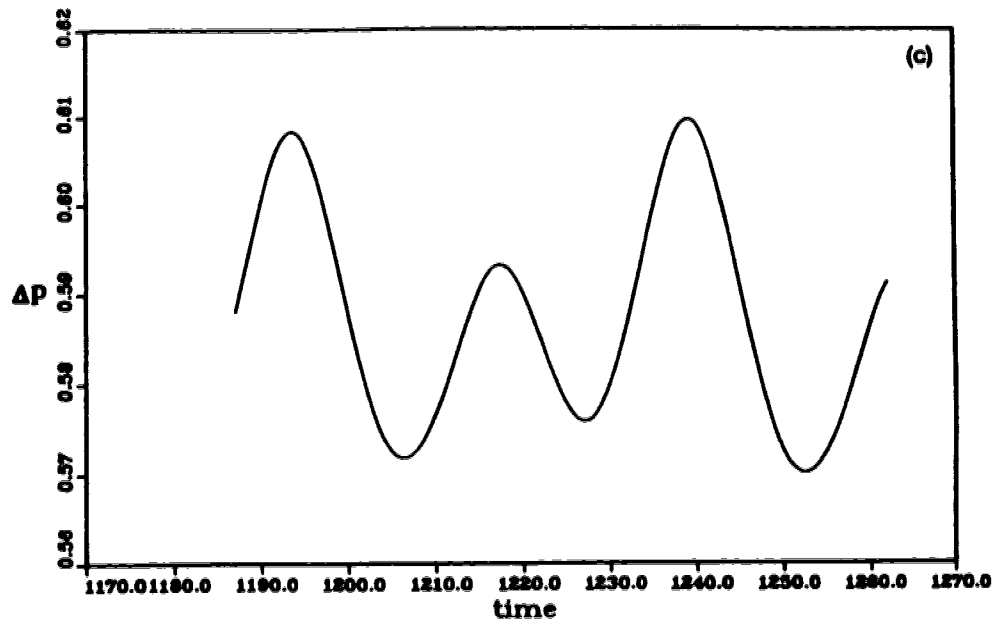Figure 2.7. (a) and (b) For caption, see page 24.

23

Figure 2.7. (a) A time record of v_z for Re = 8.84Re$_c$ used to calculate the variaton of the period T of the travelling wave (b), is shown. The velocity is sampled every time step. The corresponding record of Δp is shown in (c).
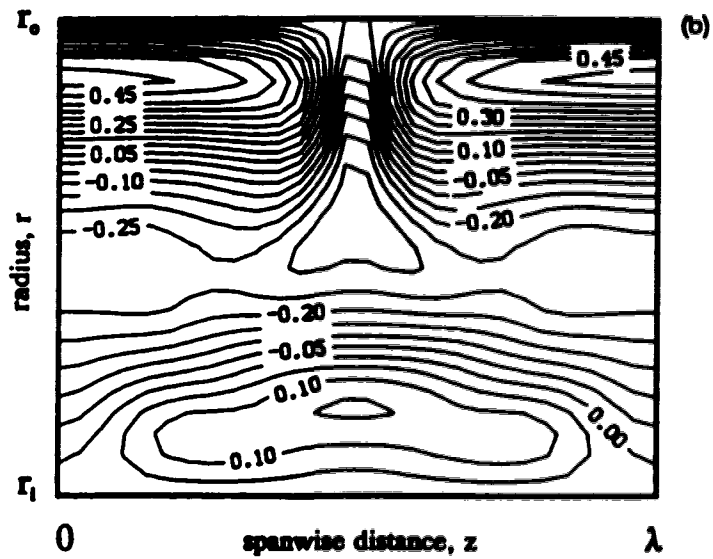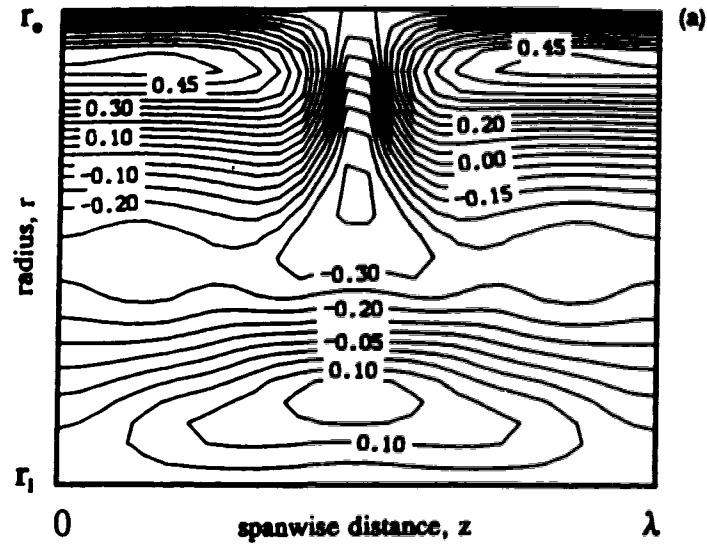
24

Figure 2.8. Contours of streamwise perturbation velocity $u_\theta = v_\theta - V(r)$ in a r - z plane averaged over one streamwise wavelength μ is shown for $Re = 8.84Re_c$; v_θ is the total velocity, and $V(r)$ is the curved channel Poiseuille flow profile. In (a) u_θ is shown at t = 1193 from Fig. 7, and in (b) at t = 1203.
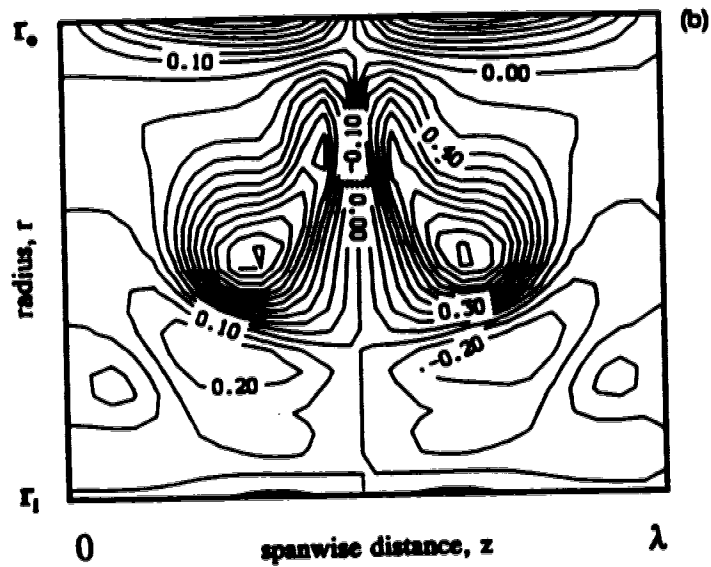
25

Figure 2.9 Contours of streamwise vorticity in a r - z plane averaged over one streamwise wavelength μ are shown for Re $=$ 8.84Re$_c$ at t $=$ 1193 in (a) and at t $=$ 1203 in (b).

26
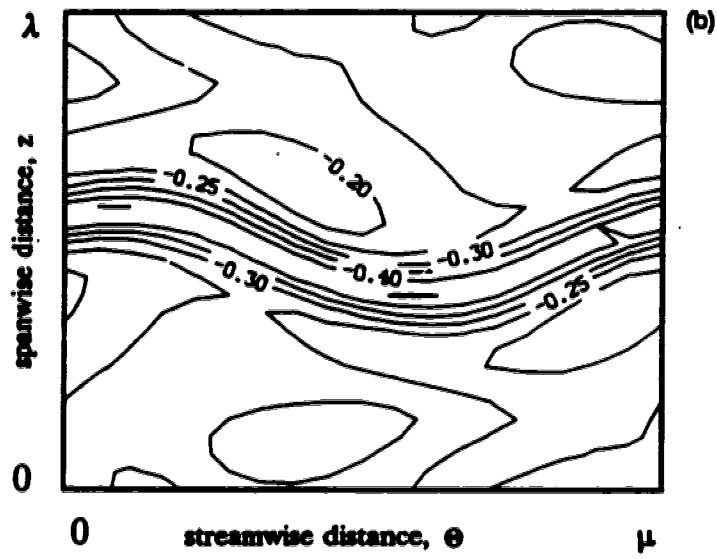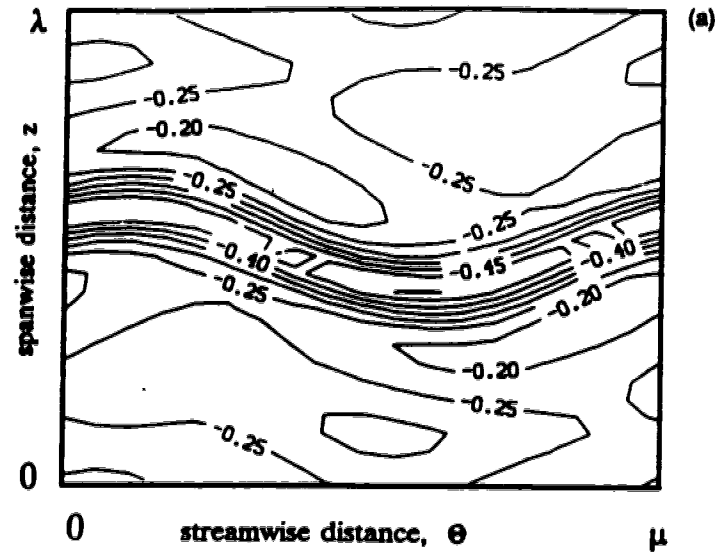
Figure 2.10 Contours of streamwise perturbation velocity u_θ in a θ - z plane at $r \sim r_c$ for Re = 8.84Re$_c$ at t = 1193 in (a) and at t = 1203 in (b).
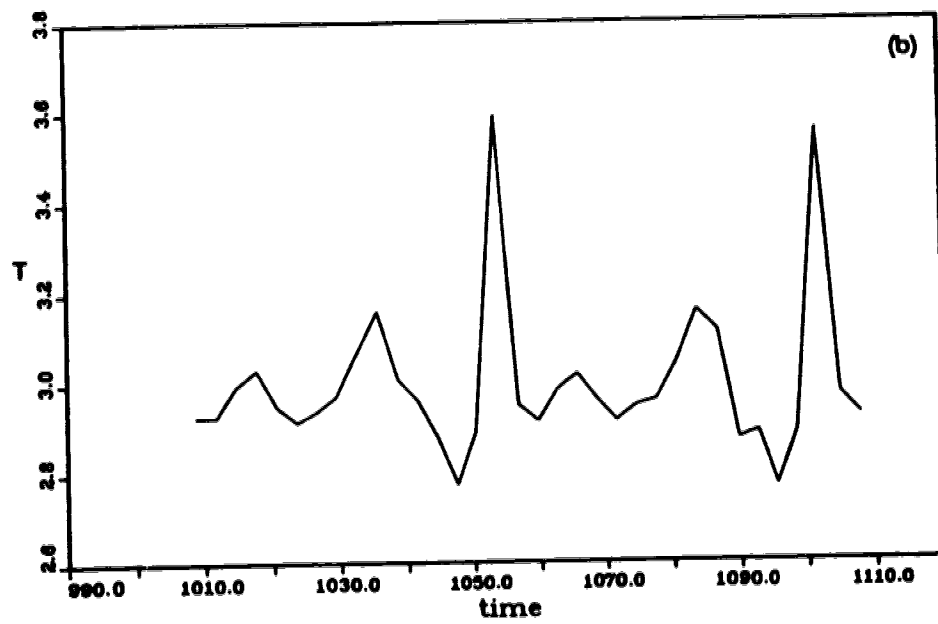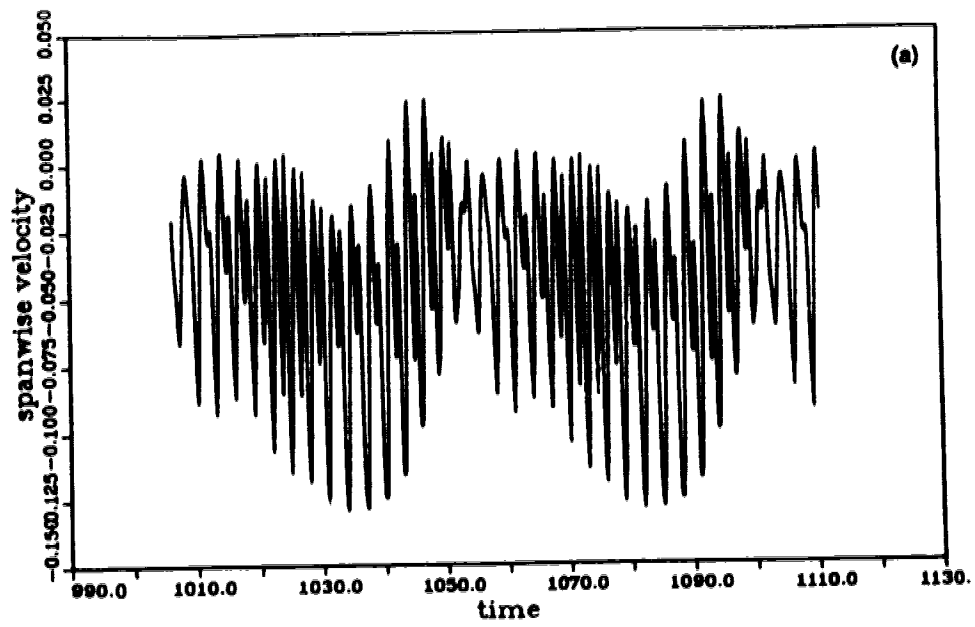
Figure 2.11. (a) and (b) For caption, see page 29 .
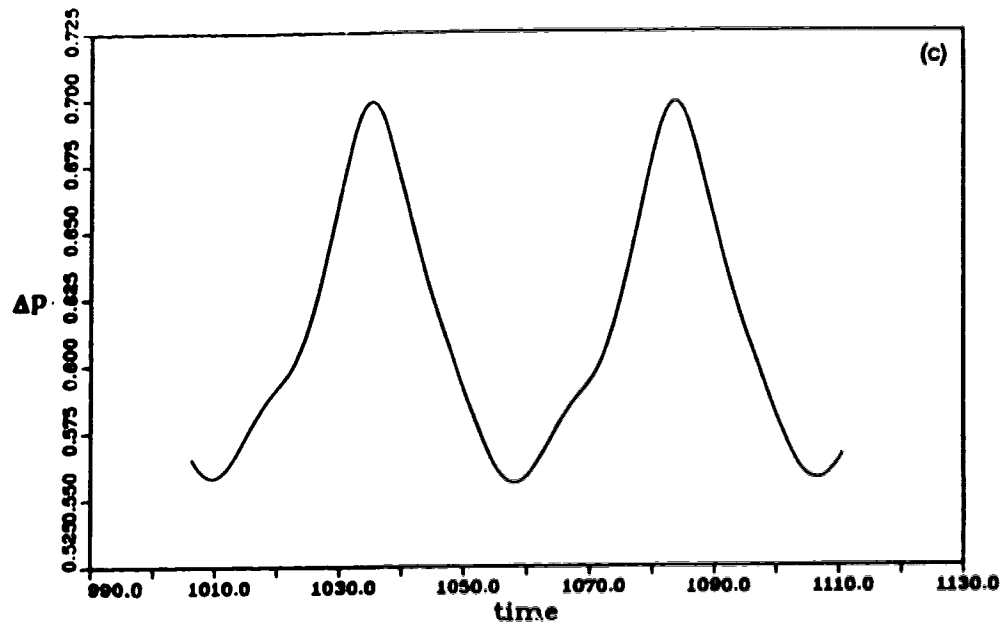
Figure 2.11. (a) A time record of v_z for Re = 10.10Re$_c$ used to calculate the variation of the period T of the travelling wave (b), is shown. The velocity is sampled every time step. The corresponding record of Δp is shown in (c).
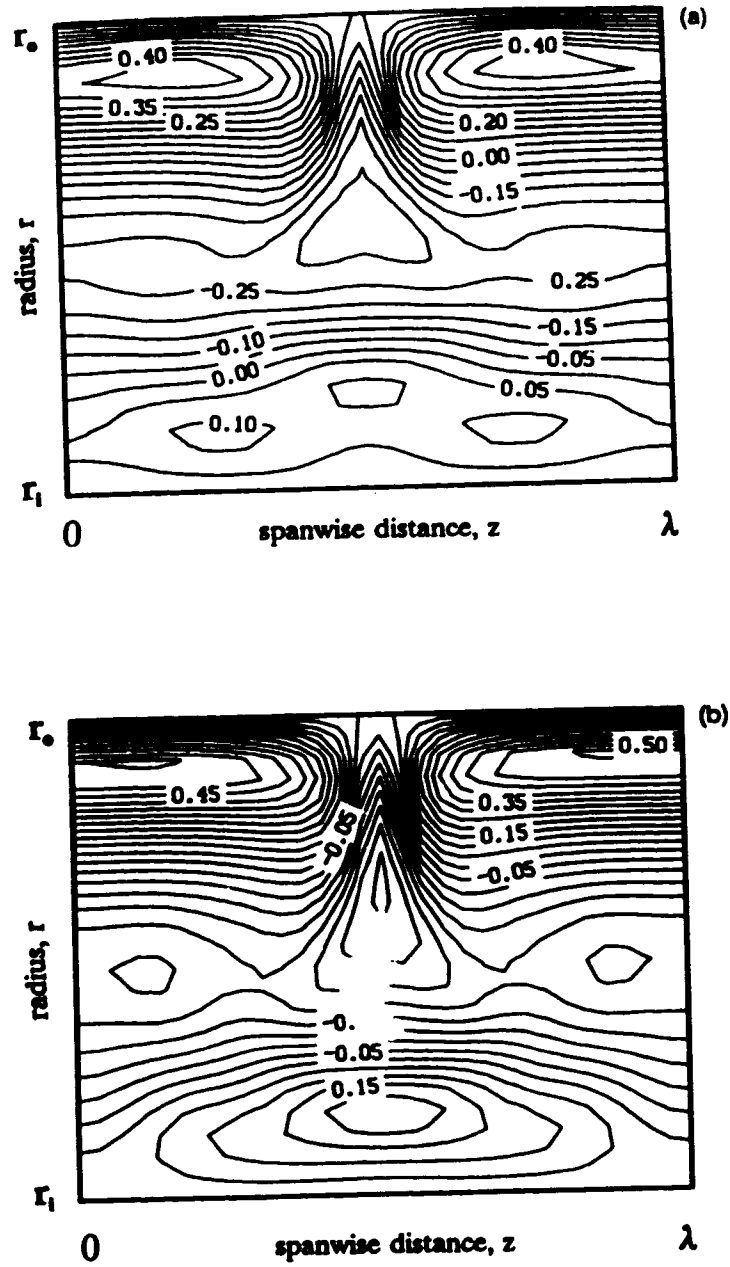
Figure 2.12. Contours of streamwise perturbation velocity u_θ in a r - z plane averaged over one streamwise wavelength μ is shown for Re = 10.10Re$_c$. In (a) u_θ is shown at t = 1057 (low Δp in Fig. 11) and in (b) at t = 1081 (high Δp).
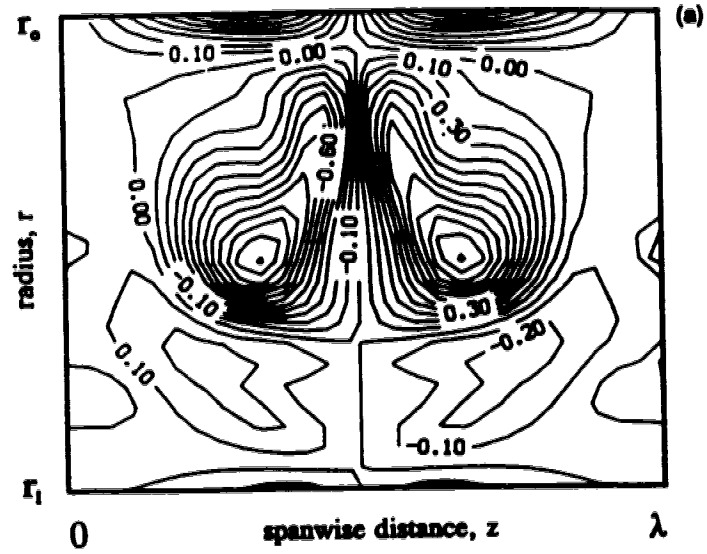
Figure 2.13. Contours of streamwise vorticity in a r - z plane averaged over one streamwise wavelength μ are shown for Re = 10.10Re$_c$ at t = 1057 in (a), and at t = t = 1081 in (b).

31

Figure 2.14. Contours of streamwise perturbation velocity u_θ in a $\theta - z$ plane at $r = r_c$ for $Re = 10.10 Re_c$ at $t = 1057$ in (a) and at $t = 1081$ in (b).
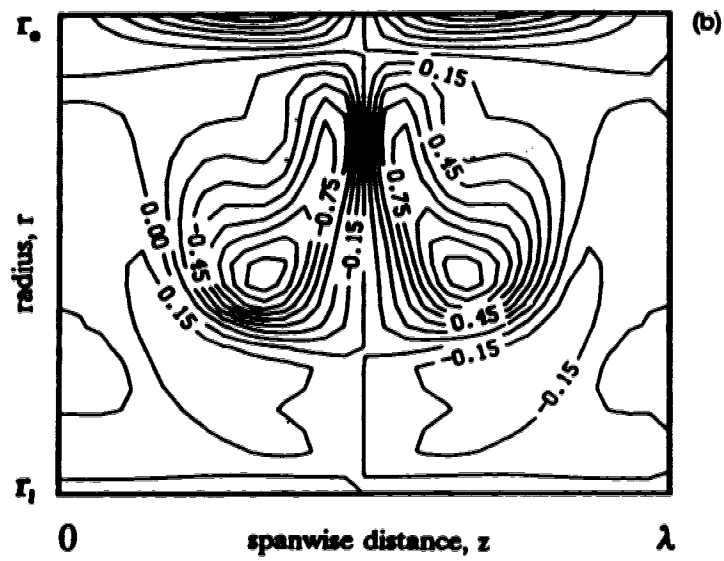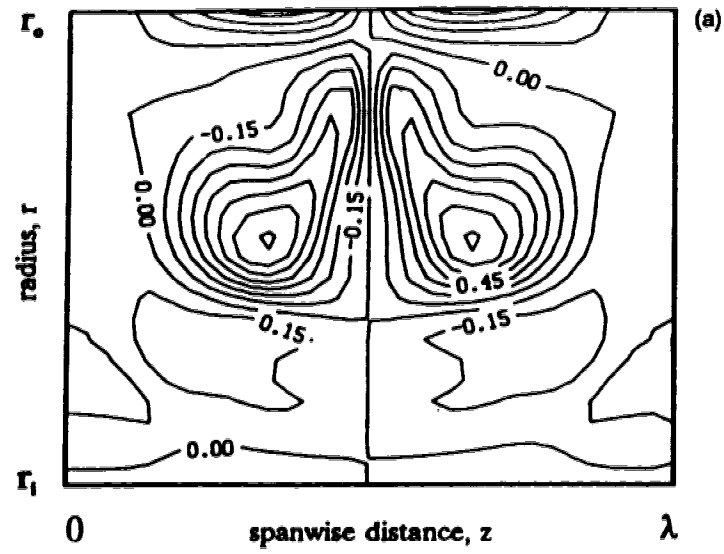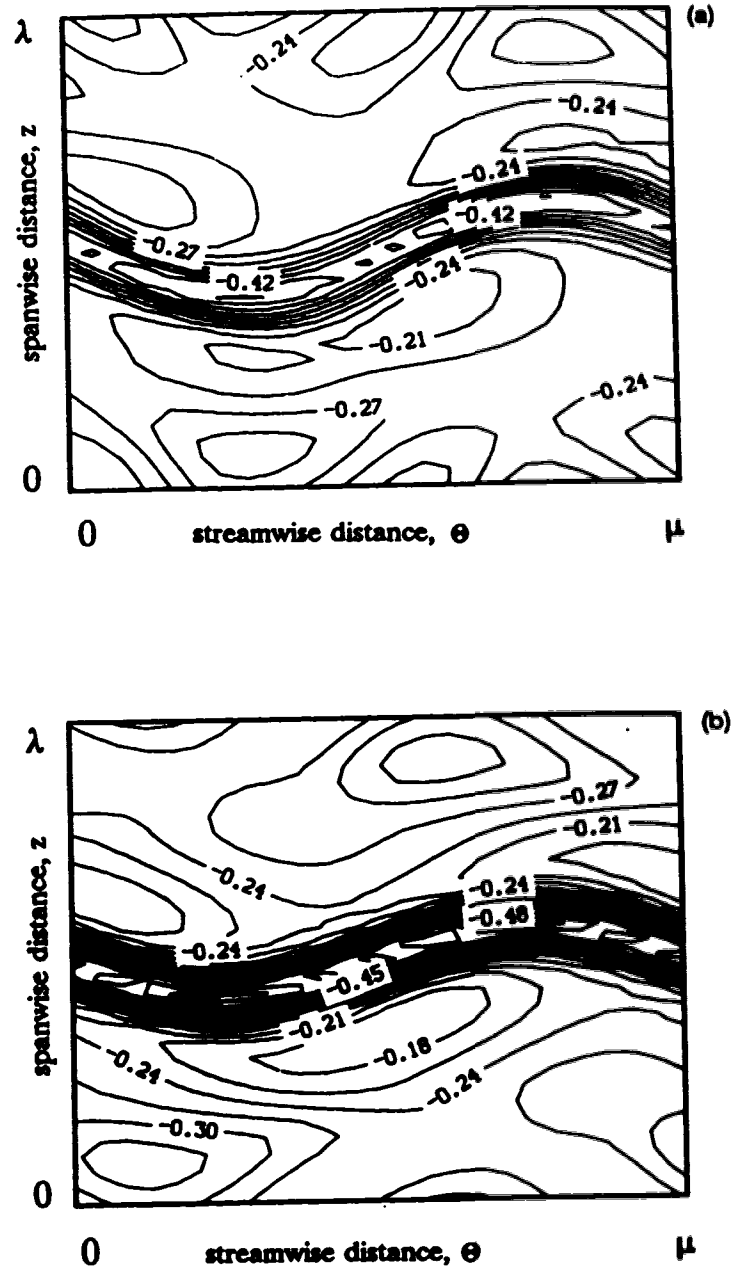
CHAPTER II REFERENCES

1. W.H. Finlay and K. Nandakumar, Phys. Fluids A 2 (7), 1163 (1990).

2. W.R. Dean, Proc. R. Soc. Lond. A121, 402 (1928).

3. W.H. Finlay, J.B. Keller, and J.H. Ferziger, J. Fluid Mech. 194, 417 (1988).

4. P.M. Ligrani and R.D. Niver, Phys. Fluids 31, 3605 (1988).

5. W.H. Finlay, P.M. Ligrani, and S.B. Bland, Submitted to Phys. Fluids A, (1990).

6. M.D. Kelleher, D.L. Flentie and R.J. McKee, ASME Trans. 102, 92 (1980).

7. I.A. Hunt and P.N. Joubert, J. Fluid Mech. 91, 633 (1979).

8. R.D. Moser, P. Moin and A. Leonard, J. Comput. Phys. 52, 524 (1983).

9. J.B. McLaughlin and S.A. Orszag, J. Fluid Mech. 122, 123 (1982).

10. R.D. Moser and P. Moin, J. Fluid Mech. 175, 479 (1987).

11. W.H. Finlay, J. Fluid Mech. 215, 209 (1990).

12. W.H. Finlay, Phys. Fluids A 1 (5), 854 (1989).

13. W. H. Finlay, Submitted to J. Fluid Mech., (1990).

14. P.S. Marcus, J. Fluid Mech. 146, 65 (1984).

15. D. Rand, Arch. Rat. Mech. and Anal. 79, 1 (1982).

16. J.P. Gollub and S.V. Benson, J. Fluid Mech. 100, 449 (1980).

17. See for instance, P. Bergé, Y. Pomeau and C. Vidal, *Order Within Chaos: Towards a Deterministic Approach to Turbulence*. (Wiley, New York, 1986).

18. Y. Guo and W.H. Finlay, Submitted to J. Fluid Mech., (1990).

19. M. Gorman and H.L. Swinney, J. Fluid Mech. 117, 123 (1982).

20. P.R. Fenstermacher, H.L. Swinney and J.P. Gollub, J. Fluid Mech. 94, 103 (1979).

CHAPTER III

CONCLUSIONS: FURTHER BIFURCATIONS AND EXPERIMENTAL

VERIFICATION OF MODULATED FLOWS

In closing, a dynamical systems view of the work is adopted in predicting what further bifurcations may occur in curved channel flow prior to becoming turbulent. As well, difficulties that may be encountered in experimentally verifying the flows discovered here are briefly discussed.

III.1 Further Bifurcations

There is current interest in the possibility that, in some cases, simple dynamical systems displaying chaotic behaviour may be useful in shedding light upon the transition to turbulence of fluid flows. Of particular interest are Taylor Couette flow and Rayleigh Bénard convection. In both cases weakly turbulent states have been described using strange attractors of low dimension[1] [2]. It is possible that curved channel flow may be similar.

Curved channel and Taylor Couette flows are similar in that in both cases the mean streamwise direction is curved. Also, the simulations performed here are closed in a similar sense that Taylor Couette flow is because of the periodic boundary conditions used in the streamwise direction. It is generally accepted that Taylor vortex flow undergoes a transition to chaos from a two frequency modulated vortex flow. Although states containing three incommensurate frequencies have been reported[3]. As well, according to the theory of Ruelle, Takens and Newhouse, three incommensurate frequencies may exist in a flow, but the associated phase space attractor will be unstable

34

and become strange[4]. For these reasons it is surprising that three incommensurate frequencies are observed in the curved channel without any chaotic behaviour. From a dynamical systems point of view of curved channel flow, it is likely that temporal chaos will ensue once the two new modes found here break out of entrainment somewhere above $Re = 10.35 Re_c$.

III.2 Possible Difficulties With Experimental Verification

Experimental verification of the modulated flows discussed in chapter II will be difficult. First, it is possible that development lengths in an experimental channel may be too short for the instabilities responsible for modulated flows to develop. Secondly, if modulated vortices exist, local splitting and merging of vortex pairs, and the convective nature of instabilities in the curved channel will complicate their identification.

In the simulations presented here, the periodic boundary conditions in the streamwise direction allow unstable perturbations to develop fully, and transients to die away completely. In the random noise initial condition run made at $Re = 8.84 Re_c$, 334 periods of ω_1, or a time long enough for the flow to circle a closed loop over 11 times, was required for the flow to become fully developed. In the run at $Re = 8.84 Re_c$ using the fully developed flow at $6.31 Re_c$ as initial condition, approximately 30 to 60 periods of ω_1 were required for full development. Experimentally, a channel with constant curvature and no helix will provide development distances less than β wavelengths long (30 periods of ω_1 in this investigation). Conditions at the channel inlet will therefore strongly affect the flow downstream.

If modulated wavy vortex flows exist, their identification may be made difficult

35

by spanwise instabilities. Even at low Reynolds numbers, splitting and merging of vortex pairs has been observed by Finlay et al.[5] to be a common event in experimental curved channel flow. The splitting and merging makes it difficult to sample velocity oscillations due to one vortex pair. This will broaden the peaks in frequency spectra and complicate the determination of fundamental frequencies. The occurrence of vortex splitting and merging increases with Re. At higher Re, it may be rare that a vortex pair will be stable long enough to observe a modulation of the travelling wave.

It is possible that streamwise instabilities are intimately related to spanwise instabilities. Thus vortex splitting and merging may be an integral part of further investigation of the transition process. If this is the case, then future numerical studies would have to include several spanwise and streamwise wavelengths in order to realistically model the flow. The runs for the results presented in here required up to 40 hours of Cray XMP CPU time. To resolve several wavelengths in the spanwise and streamwise directions for Reynolds numbers studied here is at present prohibitively expensive.

III.3 Conclusion

In chapter II the results of spectral simulations of the three dimensional, incompressible, time dependent, Navier - Stokes equations for flow through a curved channel were presented. At Re = 6.31Re$_c$ wavy Dean vortices were obtained. At Re = 8.84Re$_c$ a three frequency flow was discovered in which two nonpropagating oscillations modulate the travelling wave associated with the wavy vortices. At Re = 10.10Re$_c$ the two, new nonpropagating frequencies become phase locked, producing a modulated wavy

36

vortex flow like that observed in Taylor - Couette flow. At Re = $11.36Re_c$, a vortex doubling was encountered, limiting the extent of the present study.

The flows described here may or may not be experimentally observable, since channel inlet initial conditions will strongly affect the downstream flow. In this investigation, two strong constraints were imposed on the system: periodic boundary conditions in the spanwise and streamwise directions. Also, the flow was given a long time to develop. These conditions restrict the possible wavelengths observable and provide ample time for the flow to settle into an equilibrium state dictated by the boundary conditions. In reality the flow will have less than β streamwise wavelengths to develop (for a channel with constant curvature and no helix) and periodicity will not be enforced. The flow states described here are not incorrect however, but represent perhaps a few of many physical possibilities, and are thus useful in mapping out a physically realizable transition process.

CHAPTER III REFERENCES

1. A. Brandstater and H.L. Swinney, Physical Rev. A 35 No.5, 2207 (1987).

2. F.H. Busse, J.P. Gollub, S.A. Maslowe, and H.L. Swinney "Recent Progress" in *Hydrodynamic Instabilities and the Transition to Turbulence* ed by H.L. Swinney and J. P. Golub, Springer-Verlag, Topics in Applied Physics vol. 45.

3. L-H. Zhang and H.L. Swinney, Phys. Rev. A 31, 1006 (1985).

4. See for instance, P. Pergé, Y. Pomeau and C. Vidal, *Order Within Chaos: Towards a Deterministic Approach to Turbulence*. (Wiley, New York, 1986).

5. W.H. Finlay, P.M. Ligrani,and S.B. Bland, Submitted to Phys. Fluids A, (1990).